Article:
Soltanahmadi, S, Morina, A, van Eijk, MCP et al. (2 more authors) (2017) Tribochemical Study of Micropitting in Tribocorrosive Lubricated Contacts: The Influence of Water and Relative Humidity. Tribology International, 107. pp. 184-198. ISSN 0301-679X

https://doi.org/10.1016/j.triboint.2016.11.031

Tribochemical Study of Micropitting in Tribocorrosive Lubricated Contacts: the Influence of Water and Relative Humidity

Siavash Soltanahmadi[a*], Ardian Morina[a], Marcel C. P. van Eijk[b], Ileana Nedelcu[b], and Anne Neville[a]

*s.soltanahmadi@leeds.ac.uk

[a]iFS, School of Mechanical Engineering, University of Leeds, LS2 9JT, UK

[b]SKF Engineering and Research Centre, 3430 DT Nieuwegein, The Netherlands

Abstract

Water ingress into the lubricant as a contaminant affects performance leading to an alteration in wear, corrosion and fatigue behaviour of the tribological components especially in the rolling element bearings. The current study addresses the tribochemical phenomena involved in micropitting in tribocorrosion systems where different levels of dissolved-water are present in a model lubricant. In this study the effect of different temperatures, water concentrations and relative humidities have been investigated on micropitting under rolling/sliding contacts. The influence of free and dissolved water on tribocorrosive micropitting is clarified. The tribochemical change of the reaction films is studied using X-ray Photoelectron Spectroscopy (XPS) which confirmed that the (poly)phosphate chain length and tribofilm thickness are reduced with increased dissolved-water level.

1. Introduction

Water is known as an insidious lubricant contaminant [1, 2]. Water can enter into the lubricant through several sources including a humid environment [2-5] by absorption and condensation, leakage from heat exchanger [2], by-product of chemical reactions [2], free-water [2, 6, 7], etc.

Depending on the extent of water ingress in the oil, beyond or within the oil saturation level, water can exist as free-water or dissolved-water, respectively. The saturation level of a lubricant, representing its hygroscopicity, depends on the physiochemical characteristics of the base stock, additive package, environmental parameters (relative humidity and temperature) [8] and oil condition [9]. Free-water in the lubricant forms an emulsion which has an inferior load carrying capacity [10] leading to deficient lubricant performance.

I. Tribo-corrosive influence of water in the lubricant

Water can accelerate oil oxidation [3, 9] which in turn may increase the oil Total Acid Number (TAN) resulting in standstill corrosion and corrosion-enhanced wear and fatigue [11]. Dissolved-water can be condensed inside the microcracks through capillary effects leading to accelerated fatigue failure induced by stress corrosion cracking (SCC) [1]. Meanwhile, water contamination can favour hydrogen generation and permeation into the steel under tribological contact [12, 13] and accelerates rolling contact fatigue [14, 15] although it may not be considered as a sufficient factor to induce white etching crack [16].

The presence of water in the lubricant promotes wear incidents in steel-steel contacts under sliding [3], rolling/sliding [7] and in metal-metal contacts under fretting [4] conditions. More importantly water ingress into the lubricant is shown to promote fatigue failure where water in oil was controlled at the concentration of 100 ppm [1, 17] and to accelerate surface pitting incipient where water was dispersed in the oil in a concentration range varying between 0.5% and 2% [6]. Magalhaes et al. [18] examined the effect of water at two concentrations (1% and 5%) and reported that by increasing the lubricant contamination content (water and NaCl) depth of the pits would not increase although, fatigue life was decreased through an increase in the extent of damage.

II. Tribo-chemical influence of water in lubricant

Cen et al. [3] carried out experiments under controlled humid environments (relative humidity values of 60% and 90%) and using 1% water-containing lubricant. The results showed that changes in the bulk properties of the oil (viscosity and TAN) are negligible on addition of small amounts of water to a ZDDP-containing poly-alpha-olefin (PAO) oil [3]. This suggests that interaction of water with the lubricant additives imposes more significant changes in the lubricant performance than in the bulk oil.

Zinc Dialkyl DithioPhosphate (ZDDP), as a well-known anti-wear additive, improves the performance of the lubricant beyond its mechanical wear protection by tribofilm formation, through its anti-oxidant and partial Extreme Pressure (EP) functionality. The detrimental impact of water on the anti-wear performance of the ZDDP tribofilm has been reported in several studies [3, 6, 19]. The hydrolysis/depolymerisation of the (poly)phosphate film formed on the surface is mainly addressed as the root cause of the deleterious influence of the water on ZDDP anti-wear performance [3, 6, 20, 21]. Also, in wet clutch contacts water in lubricant

alters the tribofilm chemical composition [22] and adversely affects the frictional properties of the ZDDP-tribofilm [23] where water was added to the lubricant at a concentration of 2.9%.

The literature suggests that water as a ZDDP hydrolysis-catalyst [20], depolymerises long chain (poly)phosphates to shorter chain (poly)phosphates [6, 21] and reduces the tribofilm thickness [3, 6]. The hydrolysis effect on different types of ZDDP varies depending on their hydrolytic stability. Aryl>secondary>primary is the order of the hydrolytic stability [24]. The hydrolysis of ZDDP in the presence of water is assumed to generate alkyl sulphide and zinc phosphate [20] or olefin and phosphate acid [20]. In addition to hydrolysis impact of water on the ZDDP-tribofilm, water in oil is suggested to decay the stability of ZDDP-tribofilm through impairing the tribofilm adherence to the substrate [25].

III. The effect of ZDDP and water on micropitting

In order to improve the lubricant performance, reduce scuffing and control abrasive and adhesive wear, anti-wear additives (AW) and extreme pressure additives (EP) (S-P compounds) are used in bearings and gears lubricant formulations [26, 27]. Nevertheless, AW(s) and EP(s) under certain conditions can improve fatigue life [27-29] at low concentration [28] or can be detrimental to the fatigue life of the bearings [28, 30-32]. The high chemical activity of the reactive additives which can promote crack or pit nucleation is assumed to be the reason behind their undesirable effect on rolling fatigue life [28, 30, 31].

Furthermore, AW additives have been shown to accelerate micropitting [33-36]. ZDDP can rapidly form a tribofilm on the surface resulting in a delayed effect on proper running-in wear and increasing the probability of asperity-asperity contact. The delayed running-in, rough nature of the ZDDP tribofilm and its chemical modification in severe rolling-sliding contacts [36], which can enhance localised plastic deformation, are ascribed to be the reason behind micropitting-enhancing behaviour of ZDDP [37]. Alongside the ZDDP effect on micropitting, water contamination is also assumed to enhance micropitting wear in the bearings and gears lubricated with fully-formulated oils [38-40]. The water effect on micropitting is attributed to its destructive effect on friction-reducing and anti-wear film formation together with accelerated component surface corrosion [38, 39], although the tribochemical changes in the reaction films were not studied in detail.

The detrimental impact of water on bearings exceeds that of particle contamination under certain circumstances and affects wide range of bearings from journal to rolling element bearings. However, this effect is highly destructive where the bearings operate under severe

conditions i.e. bearings in wind turbine gearboxes. The gear teeth and bearings in wind turbine gearboxes prevalently suffer from micropitting which especially affects the bearing's functionality [40]. Water contamination is common in wind turbine gearboxes [40] especially in off- and near-shore turbines [11]. Therefore, it is significantly important to understand the influence of water on micropitting in bearings operating in demanding applications i.e. wind turbine gearbox.

Although, the detrimental effects of water on the rolling contact fatigue [1, 17, 18] and ZDDP anti-wear performance [3, 6] have been addressed, the influence of water and ZDDP-containing oil dispersion on specifically micropitting and detailed tribochemical understanding is not universally understood. Furthermore, the literature does not differentiate the impact of free-water from that of dissolved-water on micropitting. In this regard, the approach taken in the current study is to assess the tribological and tribochemical phenomena involved in the micropitting performance of water-contaminated lubricants containing ZDDP as an anti-wear additive in a specially modified tribometer for evaluating the tribocorrosion performance of lubricants.

The effect of 1 mass% water containing oil on micropitting is investigated for two different temperatures: 75°C and 90°C. Humid air with Relative Humidity (RH) values of 60% and 90% at 75°C are introduced to the test chamber in order to evaluate the effect of the dissolved-water on tribocorrosive micropitting and related tribochemical processes. A detailed investigation of the tribochemical change of the tribofilms in tribocorrosion conditions is carried out using X-ray Photoelectron Spectroscopy (XPS). The influence of free-water on tribocorrosive micropitting wear is examined through addition of 3 mass% water and inspecting the wear scars generated with 3 mass% and 1 mass% water-containing oils after 62,500 contact cycles.

2. Experimental set up

I. Micropitting tests

Micropitting wear was investigated using a modified PCS Instrument Micropitting Rig (MPR) which is schematically represented in **Figure 1**. In order to study the effect of dissolved-water, the rig is coupled with a humidifier capable of applying different RH values. The MPR rig has been described in Morales-Espejel and Brizmer et al. [34, 35].

A commercial contamination sensor, HYDAC AquaSensor AS 1000, was also employed to monitor the water saturation level in the oil. As shown in **Figure 1**, the sensor is in contact with

the lubricant inside the chamber and records the saturation concentration of water relative to the oil temperature. The sensor does not measure the water content in the oil and only records the water saturation level in the oil with respect to the fully-saturated oil (100% saturation), in a percent range varying between 0 and 100, where 100 percent saturation corresponds to the solubility limit (saturation level) of water in the oil at the certain temperature. The state of water in oil as either free-water or dissolved-water is determined using the sensor. Thereby, where the sensor shows 100%, the amount of water in oil is in excess of the saturation level and thus free-water condition exists in the lubricant. Accordingly, a percentage of less than 100 indicates that water in oil is in the dissolved-water state.

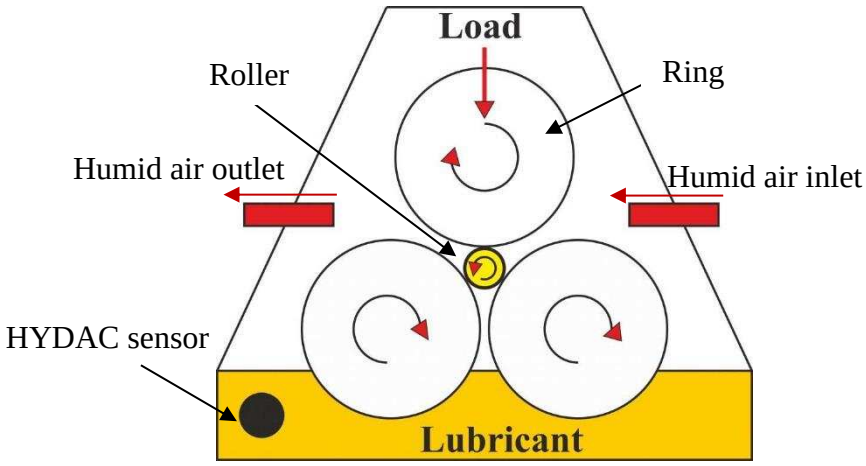

Figure 1. Schematic illustration of the MPR rig

The inspected surface is the wear scar of a steel spherical roller which is 12 mm in diameter. As shown in **Figure 1**, the roller is in the middle and undergoes cyclic load applied by three larger and equal-diameter steel counter-bodies which are inner rings of cylindrical roller bearing (designation NU209). The rings have transversely modified roughness with outside diameter of 54.15 mm after grinding. Prior to the tribological tests rollers are thoroughly washed in acetone using an ultrasonic bath. The experimental parameters in the current work are listed in Table 1.

In this study rings are carefully ground-finished transverse to the rotation-direction with the roughness of R_q=500±50 nm and rollers were circumferentially polished having a roughness value of R_q= 50±5 nm. In comparison to longitudinal or isotropic roughness of the counterbody (rings), a transverse roughness is shown to accelerate the micropitting incipient on the contact body (roller) having a smoother surface compared to counterbody in the bearings [33, 35] and gears [41]. Slide-to-roll ratio of two percent is set for the all experiments carried out in the

current study in accordance to Morales et al. [35] report showing that the slide-to-roll ratio of 0.01-0.02 can prompt the maximum surface area affected by micropitting wear.

Table 1. MPR test parameters

Specimens	Roller: 52100 steel, R_q: 50 nm, HV: 785 Rings: 52100 steel, R_q: 500 nm, HV: 745
P_{max}	1.5 GPa
Temperature	75°C and 90°C
Relative Humidity (RH) @ 75°C	Laboratory condition*, 60% and 90%
Contact cycles (on the roller)	62.5×10^3, 1×10^6
Slide-to-roll ratio (%)	2
Entrainment speed	1 m/s

*Laboratory condition: $T_{Environment}$: 20 - 25°C and $RH_{Environment}$: 40 - 65%

The test procedure includes 4 pre-contact steps which are implemented in order to achieve desired speed for rings and roller, lubricant temperature, load and slide-to-roll ratio. The steps durations are: 30 s, 900 s, 60 s and 15 s, respectively. In order to apply the desired relative humidities, the tube which is blowing humid air was connected to the chamber assembly during approx. last two minutes of the heating step as soon as the temperature was stabilised at the desired value.

II. Lubricants

The base oil employed in this study is a low-viscosity poly-alpha-olefin (PAO) base oil having kinematic viscosity of 4.0 cSt at 100°C. The water-lubricant dispersions are prepared by adding required amount of deionised water to the lubricant and mechanical shaking followed by an ultrasonic mixing making sure that water is fully dispersed in the lubricant and no noticeable deposition can be observed in the dispersion similar to the dispersing method used in Nedelcu et al. [6] report. Also, the temperature of the dispersions always was kept below 40°C during mixing to avoid considerable water evaporation. Water-containing lubricant dispersions became cloudy after mixing implying creation of an emulsion phase and existence of free-water in the lubricant. The lubricants to which water is added prior to the tests are denoted as the

lubricants with added-water further in the text. The effect of water on micropitting wear has been examined using four lubricants; details are given in **Table 2**.

Table 2. Lubricant formulation table

Lubricant formulation	Lubricant designation
PAO base oil υ= 4 cSt @100°C	BO
PAO + ZDDP (0.08 mass% phosphorus)	BO+ZDDP
PAO+ZDDP (0.08 mass% phosphorus)+(1 mass %) deionised water	BO+ZDDP+1% water
PAO+ZDDP (0.08 mass% phosphorus)+(3 mass %) deionised water	BO+ZDDP+3% water

The minimum lubricant film thickness in the contact is calculated using Hamrock-Dowson equation [42] in order to calculate Lambda ratio (λ). The lambda ratio (λ) has been defined as the ratio of the minimum lubricant film thickness to the average root-mean-square roughness of the two surfaces and is being used to identify the lubrication regime in the contact. The initial lambda ratio at the start of the contact is λ=0.04 and λ=0.05 at 90°C and 75°C, respectively which is an indication of the boundary lubricated contact.

III. Experimental approach

In the current study at first effect of two temperatures (90°C and 75°C) on micropitting wear and addition of 1 mass% of water to the lubricant at the two different temperatures after 10^6 contact cycles have been studied.

The effect of RH on tribocorrosive micropitting and the relevant tribochemistry are studied through applying two different RH values (60% and 90%) at 75°C and compared with the experiments carried out in the laboratory conditions with no added-water and with 1 mass% added-water.

It should be noted that the absolute water-vapour pressure (awvp) in the laboratory conditions ($T_{Environment}$: 20 - 25°C and $RH_{Environment}$: 40 - 65%) and at test temperature of 75°C are approx. 0.34 - 0.46 and 6 pounds per square inch (psia), respectively [43]. Therefore, change in the humidity level in the laboratory conditions (25% RH) leads to a change in RH of 1.4 - 2 % at the test conditions, which is negligible.

Controlling RH at 90°C and subsequent potential condensation is arduous in the current experimental set-up which makes the results contentious. In this regard, the effect of dissolved-water through absorption from humid air is only studied at 75°C. The water concentration in oil after each test was measured by Karl Fischer Titration.

In order to assess the impact of free-water on tribocorrosive micropitting, tests are carried out with 62.5×10^3 contact cycles and different added-water concentrations (1 mass% and 3 mass%). The data acquired from water saturation sensor showed that only after 90 seconds of the tribological contact (~7×10^3 contact cycles), due to the water evaporation, water saturation level is below 100% for the lubricant with initial addition of 1 mass% water. This suggests that most of the contact cycles performed under dissolved-water for the rollers lubricated with BO+ZDDP+1% water.

While the roller lubricated with 1 mass% water-containing oil experienced ~7×10^3 contact cycles under free-water condition, the roller lubricated with 3 mass% water-containing oil tolerated all 62.5×10^3 contact cycles under free-water condition. Therefore, the roller surface lubricated with BO+ZDDP+3% water and undergone 62.5×10^3 contact cycles represents the impact of free-water on micropitting. In the interpretation phase, the tribocorrosive and tribochemical effect of water on micropitting were addressed using white light interferometry (WLI), scanning electron microscopy (SEM), and optical microscopy and x-ray photoelectron spectroscopy (XPS), respectively.

3. Surface analysis techniques

I. Wear scar observation

The wear scar profile has been obtained utilising Bruker's NPFLEX based on Wyko (white light interferometry (WLI)) technology. The wear scar profiles of four spots of each specimen have been generated. In this study attempts have been made to produce a well-representative map from micropitted area in the wear scar on the surface of the roller by the implementation of the Multiple Region (MR) data analysis technique which has been incorporated in the Vision64 software. The scanned WLI images of the wear scars are analysed using MR analysis with the minimum data pixel size set to 10. In order to screen the real data from data generated through software error, the data which are smaller than 10 μm^2 in surface area were excluded from the further analysis. Following careful MR analysis the total micropitted surface area on the scanned WLI images are calculated through summing up the identified discrete micropitting regions. This process schematically is shown in **Figure 2**. The average of measurements from three different specimens are reported as the average micropitted surface area. Optical images from wear scars are also captured in order to inspect the wear scars of the specimens lubricated at different water concentrations.

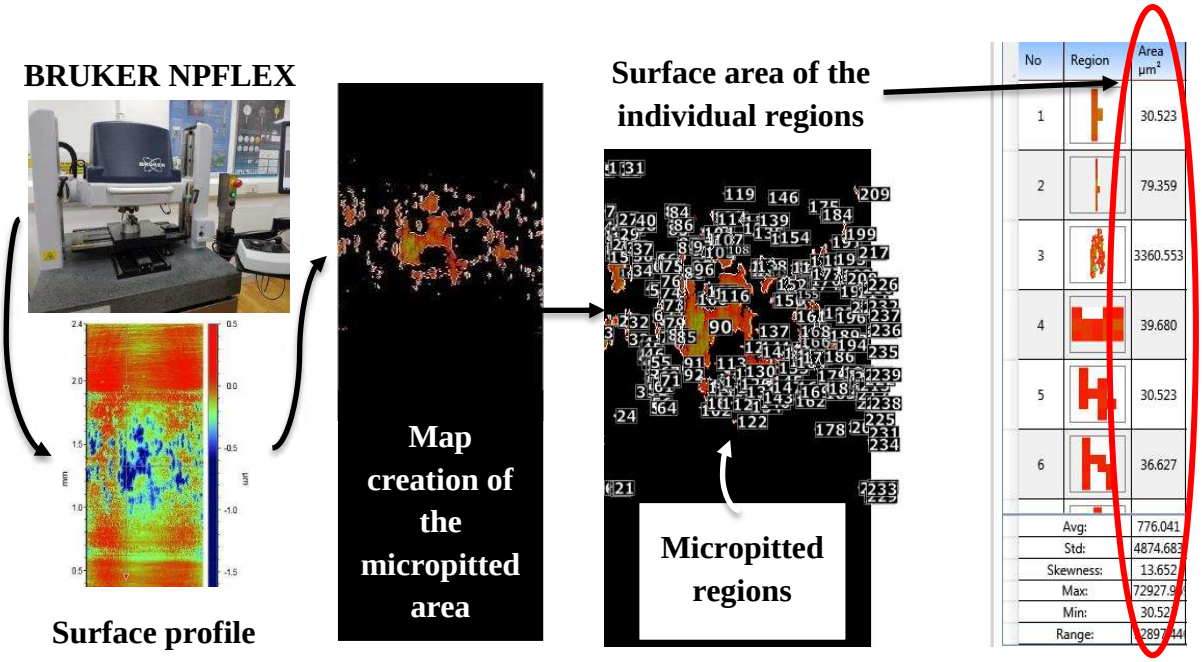

Figure 2. Illustration of micropitted surface-area measurement using multiple region analysis

A Zeiss Supra 55 SEM is employed to capture images from the wear scars. A secondary electron detector used in order to observe the surface morphology in details. The secondary electrons emitted from the specimen have been excited by the electrons coming from the electron-gun having acceleration voltage of 5 kV. A washing procedure of tissue wiping using acetone followed by ultrasonic cleaning in acetone for 30 minutes has been conducted prior to WLI and SEM analysis in order to remove residual oil and reaction film from the surfaces.

II. Chemical investigation of the reaction film

X-ray Photoelectron Spectroscopy (XPS) surface analysis is conducted to investigate the chemical composition of the tribofilm and assess tribofilm thickness. A PHI 5000 Versa Probe™ spectrometer (Ulvac-PHI Inc, Chanhassen, MN, USA) which uses a monochromatic Al Kα X-ray source (1486.6 eV) is employed for this purpose.

The residual lubricant has been cleaned out the surface prior to the XPS analysis through flushing n-heptane followed by an ultrasonic cleaning in n-heptane for three minutes.

In order to identify inside and outside of the tribological contact, survey spectra were collected from different locations with an energy step size of 1 eV. The detailed spectra have been collected from the wear scars approximately at the centre with a beam size of 100 µm and a power of 23.7 W in the fixed analysed transmission mode. The energy step size of 0.05 eV for the oxygen, iron, phosphorous and sulphur acquisition and 0.1 for carbon and zinc have been selected.

Using CASAXPS software (version 2.3.16, Casa Software Ltd, UK), the detailed XPS spectra were fitted with Gaussian–Lorentzian curves after subtracting a Shirley background. Aliphatic carbon Binding Energy (BE) is referred to 285.0 eV in order to correct the charging effect of beam on specimens. In accordance with spin-orbit splitting, area-ratio-constraint of 2:1 for the two components of the signal ($p_{3/2}$ and $p_{1/2}$) has been considered to perform phosphorous (P 2p) and sulphur (signal S 2p) signal fitting [6, 44]. Also, position-difference-constrain of 0.85 eV and 1.25 eV is applied for the two components of the phosphorus and sulphur signals, respectively[6]. The detailed spectra from Zn Auger ($L_3M_{4,5}M_{4,5}$) signal were collected and fitted using two peaks in order to extract two signals (^1G and ^3F) [45]. Modified Auger parameter (α') was calculated using Zn $2p_{3/2}$ BE and Zn $L_3M_{4,5}M_{4,5}$ ^1G Kinetic Energy (KE) signals.

Following detailed analysis of the tribofilm top surface, the tribofilm is sputtered using an Ar^+ ion source (2 keV energy, 2 ×2 mm^2 area and 1 μA sputter current), in order to estimate the tribofilm thickness and observe the elemental distribution of the tribofilm across its depth. The ion sputtering performed every 60 s followed by XPS detailed acquisition after each sputtering. The rate on steel was found to be 4.5 nm per minute by Wyko [6]. The sputtering time at which the concentration of O1s signal becomes less than 5% and traces of the tribofilm elements (Zn, P, S) is not found in the detailed spectra, is considered as a measure of the reaction layer thickness [6].

4. Results

I. The effect of added-water and temperature on micropitting

Following the sample washing procedure to remove the reaction layer, WLI images are scanned from the wear scar on the roller surfaces. The effect of 1 mass % added-water on micropitting at two different temperatures of 90°C and 75°C are shown in **Figure 3** and **Figure 4**, respectively. The generated micropitting maps from the wear scars using Multiple Region (MR) analysis are shown on the right hand-side of the corresponding WLI wear scar profiles.

As can be seen in **Figure 3** and **Figure 4** the generated micropitting maps effectively represent the micropitted regions in the wear scar. The calculated micropitting surface areas are indicated in the lower part of the corresponding micropitting maps. The average micropitted surface area from measurements on three specimens are calculated and indicated in **Figure 3** and **Figure 4** (e and f).

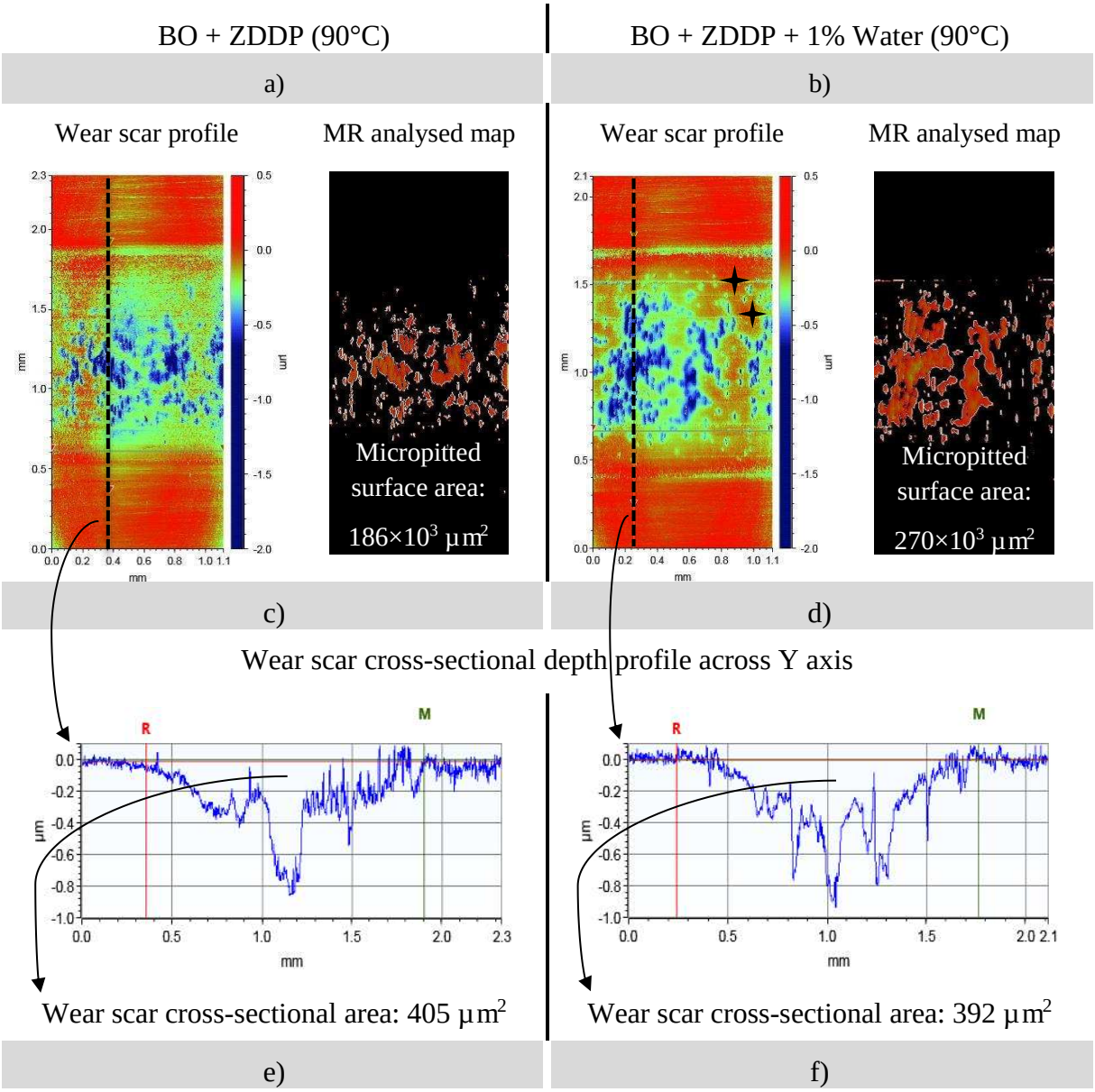

Figure 3. Wear scar and MR profile, corresponding wear scar depth profiles and average micropitted surface area of the roller surfaces lubricated with a,c,e) BO + ZDDP and b,d,f) BO + ZDDP + 1% Water at 90°C. R and M are the profile cursors which are placed at the wear track edges ✦ Abrasive marks

The wear scar cross-sectional depth profile corresponding to the black dashed line on the wear scar profile of the rollers lubricated with BO + ZDDP and BO + ZDDP + 1% water are shown below the wear scar profiles in c and d section of the figures, respectively. The surface areas of the wear scar cross-sectional depth profiles are indicated below the corresponding depth profiles. The wear scar cross-sectional area is a representative of the extent of the material loss which is induced on the roller surfaces due to the tribological contact.

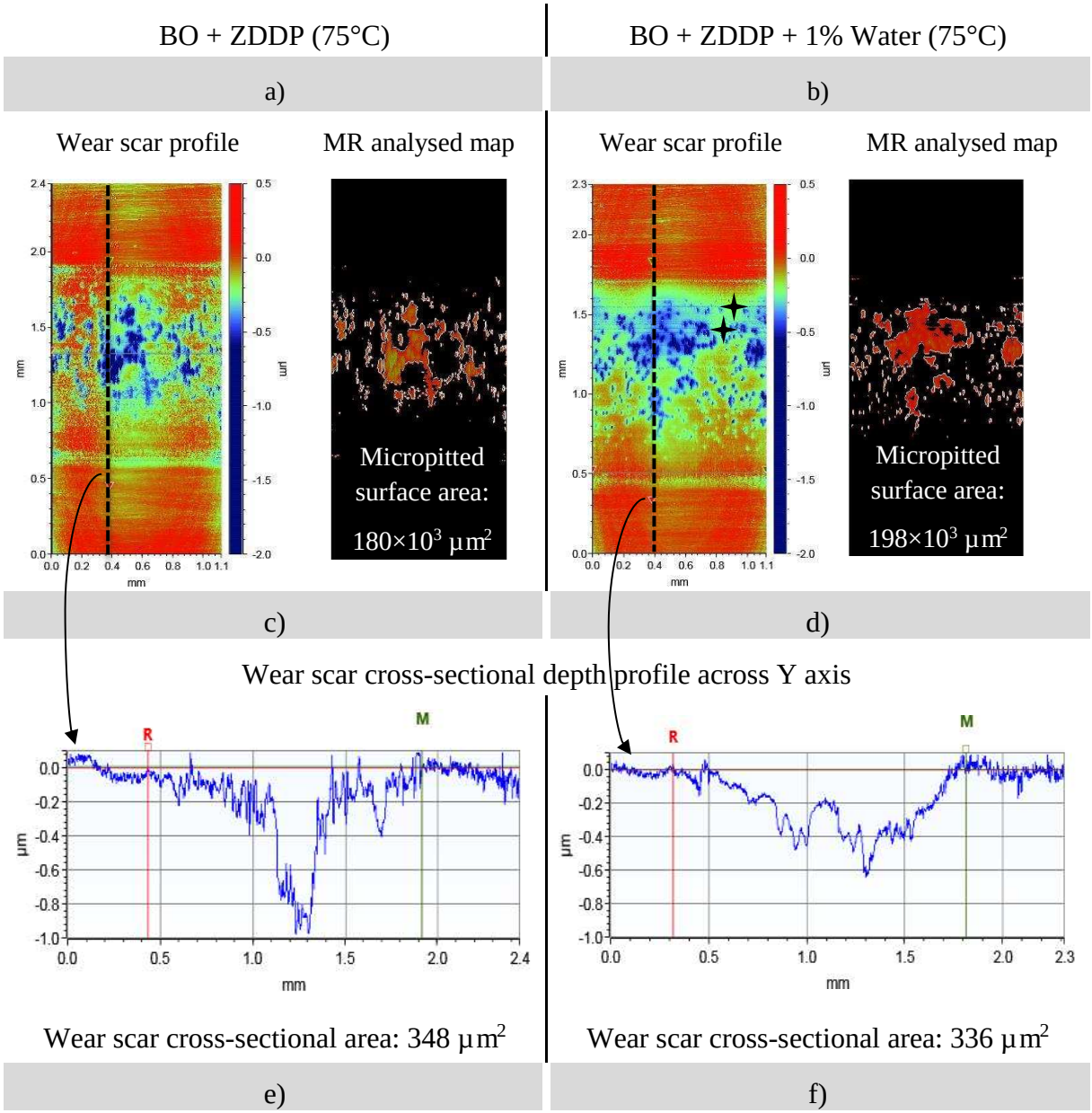

Figure 4. Wear scar and MR profile, corresponding wear scar depth profiles and average micropitted surface area of the roller surfaces lubricated with a,c,e) BO + ZDDP and b,d,f) BO + ZDDP + 1% Water at 75°C. R and M are the profile cursors which are placed at the wear track edges ✦ Abrasive marks

A clear increase in micropitting can be observed on the roller surfaces lubricated with added-water. The 1% of added-water increases the micropitted surface area by approx. 15% and 25% for the experiments carried out at 90°C and 75°C, respectively. There is an approx. 30% increase in micropitting of BO + ZDDP lubricant when the experiments are performed at 90°C compared to the experiments performed at 75°C. A considerable rise in the wear scar cross-sectional areas at 90°C compared to 75°C suggests that material loss at higher temperature is

increased. The increase in micropitting and material loss can be expected at higher temperature (90°C) due to the increase in the severity of the contact which is resulted from the lower viscosity of the oil at 90°C with respect to 75°C and consequent inferior lambda ratio. In addition, an accelerated ZDDP-tribofilm formation at 90°C compared to 75°C enhances micropitting on the surface [33]. Abrasive marks can be observed on the wear scars of the surfaces lubricated with added-water. The abrasive marks on the wear scar profiles are designated in the images using a black-filled star symbol.

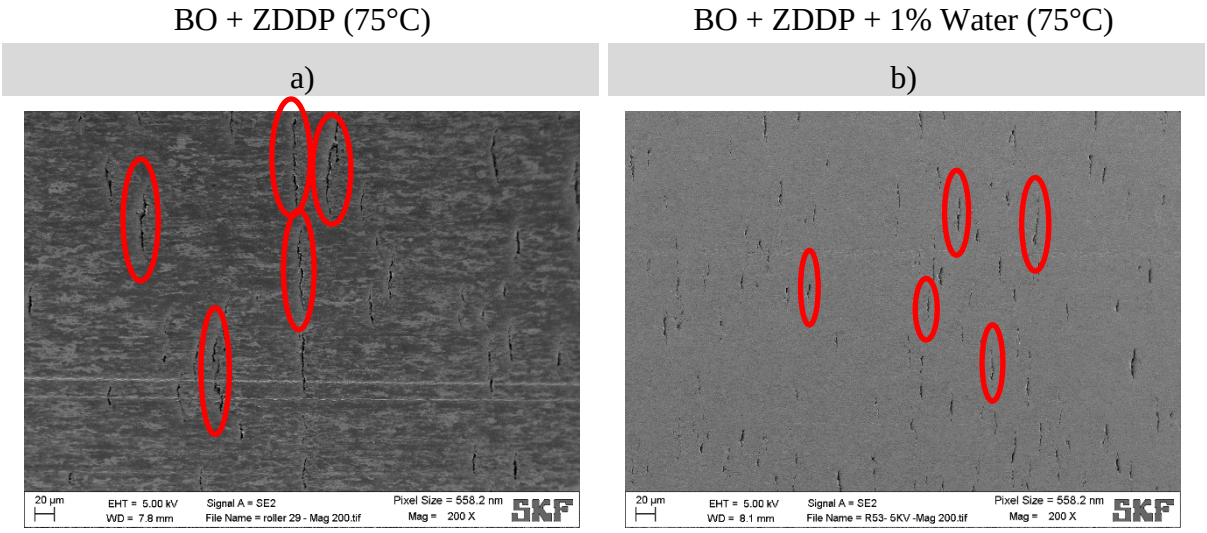

Figure 5. SEM images of the roller surfaces lubricated with a) BO + ZDDP and b) BO + ZDDP + 1% Water at 75°C

The wear scar cross-sectional depth profiles of the rollers lubricated with BO+ZDDP formulation are shown in **Figure 3** (c) and **Figure 4** (c) suggesting shallow wear track at edge containing deep and large discrete micropits concentrated in the middle of the wear scar which is within the zone with highest contact pressure. In contrast, the rollers lubricated with added-water (**Figure 3** (d) and **Figure 4** (d)) have a deeper wear scar depth profile at the edges, suggesting **mild wear** on surface, with more initiated micropits, which are spread out across the wear scar, compared to that of BO+ZDDP. Therefore, BO+ZDDP formulation protected surface from mild wear while inducing large micropits and BO+ZDDP+1%water induces larger wear and greater micropitted surface area.

Furthermore, comparing **Figure 3** a with b, **Figure 4** a with b and **Figure 5** a with b, it can be observed that while micropitting surface area is increased on the rollers lubricated with added-water, the dimensions of the discrete micropits are smaller. This suggests that the material loss in the case of contacts lubricated with the added-water is generated through enhanced

micropitting nucleation and mild wear, while the material loss in the case of contact lubricated with BO+ZDDP is mainly induced through **micropitting initiation** and **propagation**.

II. The effect of relative humidity on micropitting

The effect of two different relative humidities (60% and 90%) on micropitting is shown in **Figure 6**. The wear scars are extensively micropitted across the whole wear track. The micropitted surface area of the roller lubricated under 60% of RH is close to that of BO+ZDDP+1%water lubricated surface. The micropitted surface area of the roller lubricated under 90% of RH increased by more than 60% compared to the laboratory conditions. Also, abrasive marks become more intense by increasing the RH to 90%. Similar to what is observed in the case of 1% added-water, the rollers lubricated under humid environments have a deeper wear scar depth profile at the edges as shown in **Figure 6** (c and d) and show mild wear incident on the roller surfaces. **Figure 7** shows the SEM images of the wear scars generated in laboratory and 60% of RH conditions which confirms enhanced micropitting initiation and micropitting surface density in the case of 60% of RH.

In **Figure 8,** the water saturation, which is recorded by the Hydac sensor, is shown throughout the pre-contact and contact durations. Also, water concentration after each test, measured by Karl Fischer Titration, is indicated in **Figure 8** (b). The pre-contact step which includes sub-steps of achieving the desired speed for rings and roller, lubricant temperature, load and slid-to-roll ratio, is plotted in black colour. The first 62.5×10^3 contact cycles for the lubricants with the added-water is plotted in red colour.

As can be seen in **Figure 8** (a), data acquired from water saturation sensor show that the most of the water in the lubricant with 1% of the added-water is evaporated during the pre-contact steps specifically heating step and only approximately 7×10^3 contact cycles are carried out under the free-water condition and most of the tribological contact is progressed under the dissolved-water condition.

The Karl Fischer measurements are well in agreement with the sensor records. The dissolved-water concentration in the lubricants reached a steady state condition after 250×10^3 contact cycles. The data from the sensor and the Karl Fischer measurements show that the relative order of increasing dissolved-water concentration for a series of test conditions is BO + ZDDP (RH 90%) > BO + ZDDP + 1% Water > BO + ZDDP (RH 60%) for the tests conditions used in this study.

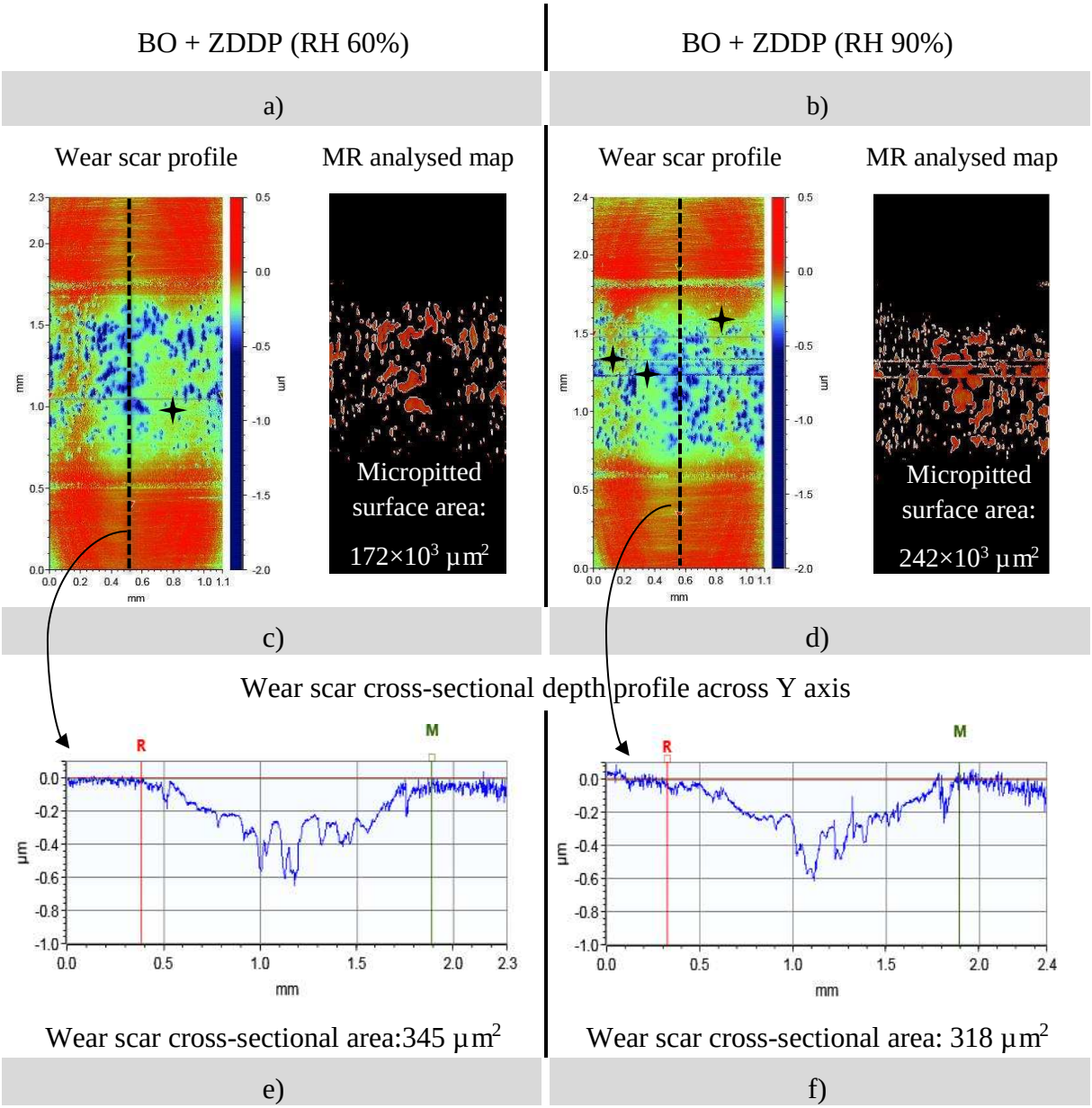

Figure 6. Wear scar and MR profile, corresponding wear scar depth profiles and average micropitted surface area of the roller surfaces lubricated with a,c,e) BO + ZDDP (RH 60%) and b,d,f) BO + ZDDP (RH 90%) at 75°C. R and M are the profile cursors which are placed at the wear track edges ✦ Abrasive marks

Furthermore, the micropitted surface area and abrasive marks increase along the series of test conditions BO + ZDDP (RH 90%) > BO + ZDDP + 1% Water > BO + ZDDP (RH 60%). This suggests that an increase in the dissolved-water concentration brings about an enhancement in micropitting and abrasive wear. **Figure 9** a and b compare the micropits induced on the wear scars on the roller surfaces lubricated with BO + ZDDP (RH 60%) and BO + ZDDP + 1% Water, respectively.

BO + ZDDP	BO + ZDDP (RH 60%)
a)	b)

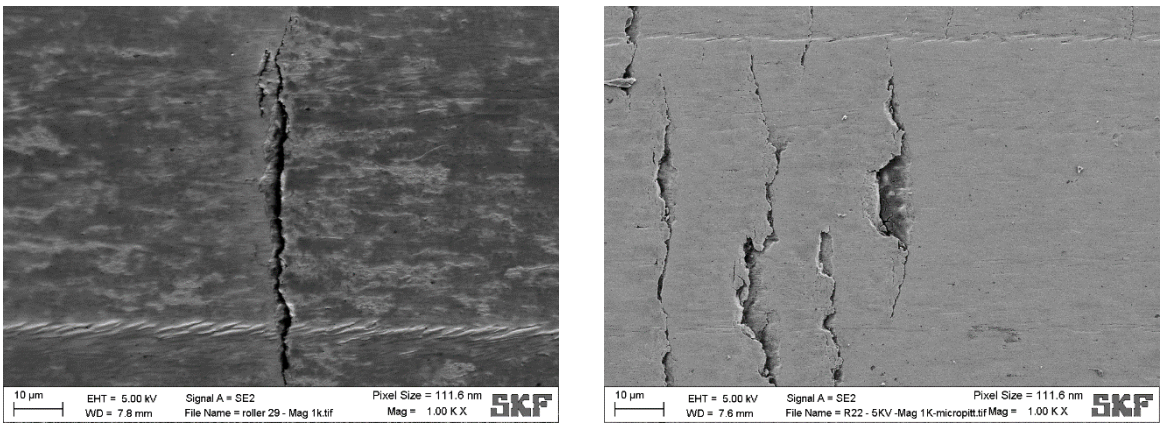

Figure 7. SEM images of the roller wear scars lubricated with a) BO + ZDDP and b) BO + ZDDP (RH 60%) at 75°C

The appearance of micropits is similar and show that the micropits propagate opposite to the sliding direction into the bulk of the material in agreement with Oila et al. [46] and also transverse to the rolling/sliding direction.

a) Water contamination sensor record	b) Karl Fischer measurement

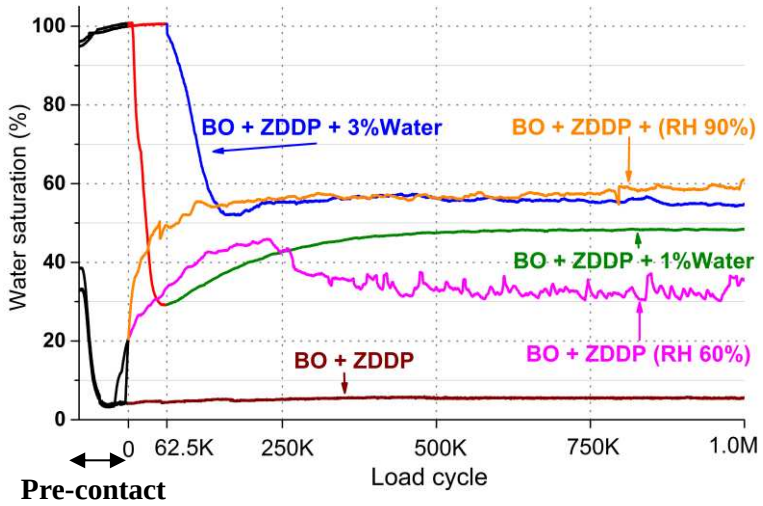

Water concentration after 1 million contact cycles (mass%)	
BO + ZDDP + 3% Water	0.021 ± 0.001
BO + ZDDP + 1% Water	0.017± 0.001
BO + ZDDP (RH 90%)	0.022 ± 0.001
BO + ZDDP (RH 60%)	0.013 ± 0.001

Figure 8. a) Water saturation level measured by Hydac contamination sensor and b) water concentration of the oils after the tests

In the **Figure 9** (a) microcracks can be observed inside the micropits on the crack faces which can be an indication of a crack branching which is typical for the tests conditions used in this study.

BO + ZDDP (RH 60%)	BO + ZDDP + 1% Water
a)	b)

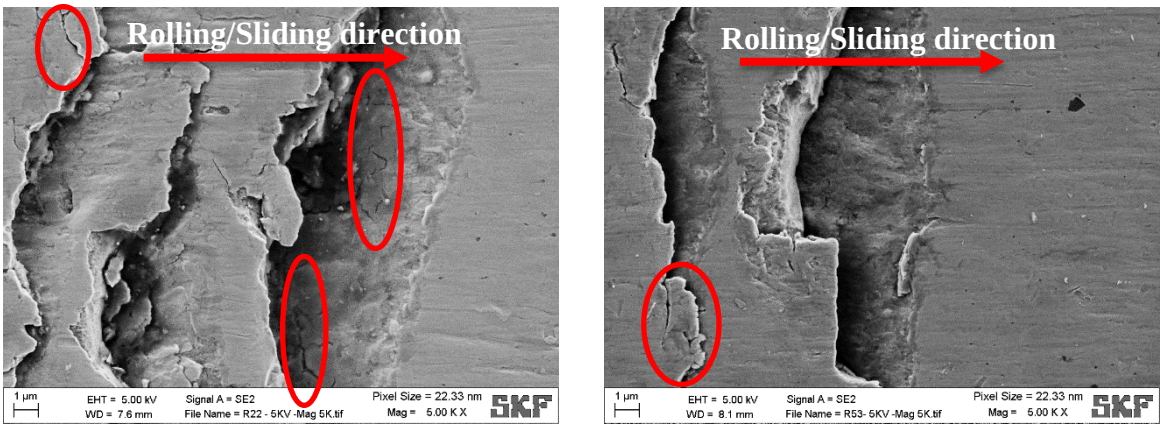

Figure 9. SEM images of the micropits appearance on the wear scars

III. The effect of free-water on micropitting

The effect of free-water on micropitting has been investigated through adding 1% and 3% water and inspecting the roller surfaces after 62.5×10^3 contact cycles and comparing with the roller surface lubricated with BO + ZDDP lubricant formulation without added-water (**Figure 10**). The change in the water saturation level of the lubricant containing 3% of added-water is displayed in **Figure 8** (a) which shows that the saturation level of the lubricant remains 100% during first 62.5×10^3 contact cycles. Therefore, 3% of added-water propelled the contact under free-water condition throughout 62.5×10^3 contact cycles. Whilst, roller lubricated with BO + ZDDP + 1%water and experienced 62.5×10^3 contact cycles, has been under tribological contact in the free-water condition for approximately 11% of its tests duration. Optical images taken from the wear scars of the rollers lubricated with BO + ZDDP, BO + ZDDP + 1%water and BO + ZDDP + 3%water after 62.5×10^3 and 1×10^6 contact cycles are shown in **Figure 10** (a) and (b), respectively.

As can be seen in **Figure 10** (a) the wear scar of BO + ZDDP has discrete micropits on surface and no sign of abrasive wear can be observed. In the wear scar of roller lubricated with BO + ZDDP + 1%water, micropits and an abrasive mark are visible. The micropitting density is less compared to BO + ZDDP lubricated roller, considering that approximately 11% of the test duration was in the free-water condition. However, on the wear scar of BO + ZDDP + 3%water, which is lubricated in the free-water condition throughout the test duration (62.5 K cycles), there is no trace of abrasive wear and only few and insignificant micropits are visible. Most probably, the negligible micropits on the surface of BO + ZDDP + 3%water lubricated roller

are generated after the actual test and within the stopping-step in which the un-loading takes place and rotation of the specimens is gradually halted. The stopping-step is completed approximately two minutes after the actual test which provides the lubricant with the required time to go through a transition from free-water to dissolved-water condition.

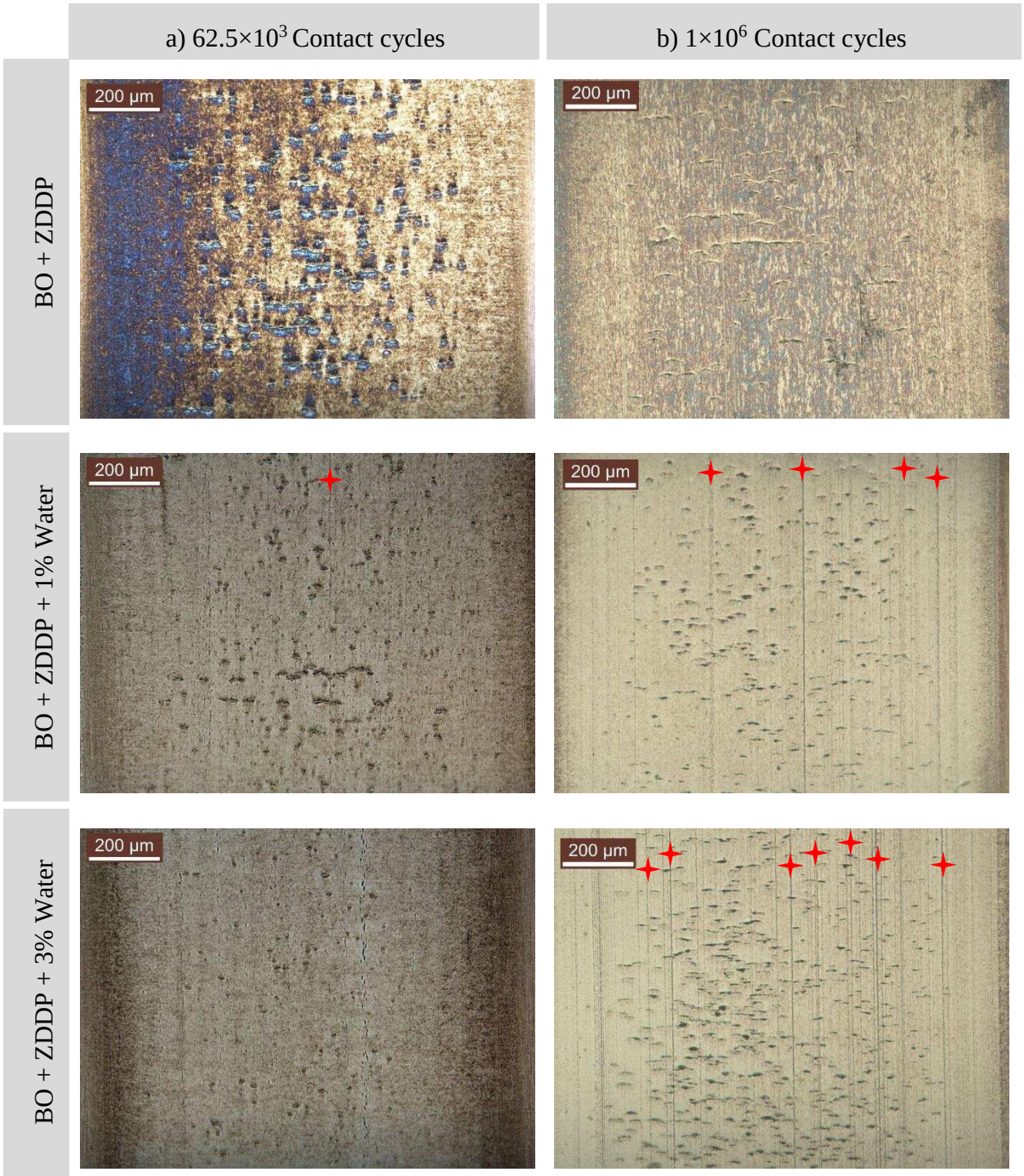

Figure 10. Optical images of the wear scars on the rollers after a) 62.5×10^3 and b) 1×10^6 contact cycles. ✦ Abrasive marks

In **Figure 10** (b), which shows the wear scars rollers after 10^6 contact cycles, the micropitting and abrasive wear are enhanced in the case of lubricants with added-water. The micropitting and abrasive wear are also increased with an increase in the water concentration to 3% which is due to the increase in the dissolved-water concentration as shown in **Figure 8**. This suggests that free-water profoundly favours mild wear process and subsequently micropitting is hindered. On the other hand, dissolved-water facilitates mild wear and significantly enhances micropitting initiation and abrasive wear simultaneously.

IV. Tribochemistry in presence of water in oil and humidity

IV.I Chemical composition of the tribofilm top layer

In **Figure 11** the detailed XPS spectra of the C 1s, O 1s, P 2p, Zn 3s, Fe 2p, S 2p and Zn $L_3M_{4,5}M_{4,5}$ for the roller lubricated with BO + ZDDP (RH 60%) are shown.

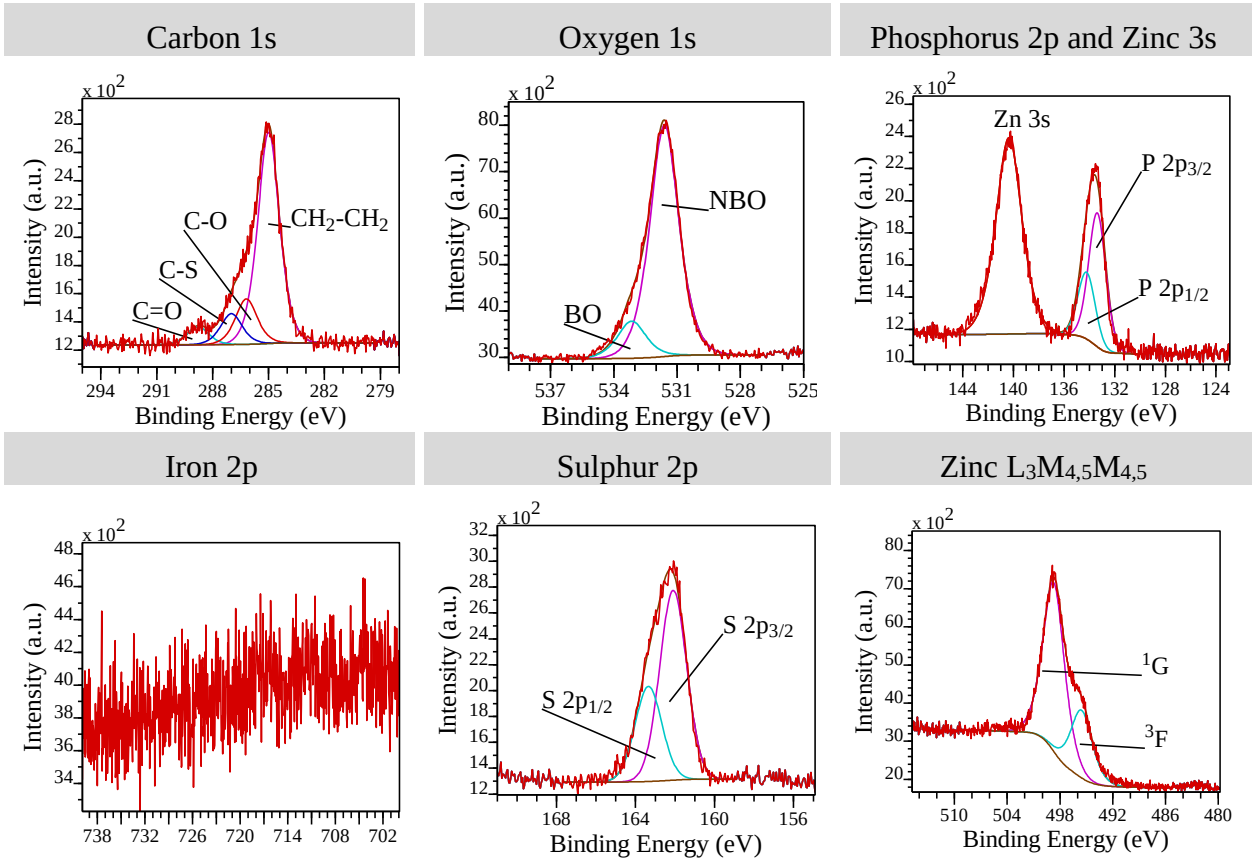

Figure 11. XPS detailed spectra of the ZDDP-tribofilm elements in the wear scar of the roller lubricated with BO + ZDDP (RH 60%)

All other spectra from other roller surfaces were fitted using the same curve-fitting procedure. The details of the fitted spectra are listed in **Table 3.** The carbon C 1s spectra collected from the wear scars are resolved to four signals. The main signal appeared at 285.0 eV assigned to the aliphatic carbon (C-C and C-H). The three other minor contributions exhibited at around

286, 287, and 289± 0.1 eV which are attributed to C-O, C-S and C=O (carbonate and/or carboxylic), respectively. The O 1s signal consists of two peaks in the wear scars. The most intense peaks were found at 531.4 - 531.6 ± 0.1 eV assigned to Non-Bridging Oxygen (NBO) from phosphate chain (-P=O and P-O-M; where M is metal: Zn) and from carbonates and hydroxides [6, 47]. The second contributions to O 1s signals appeared at 532.8 – 533.1 ± 0.1 eV correspond to Bridging Oxygen (BO) from the phosphate chain (P-O-P). No metal oxide peak at 529-530.7 eV and iron signal are detected in the XPS spectra collected from the top layer of the ZDDP-tribofilm (see **Table 3** and **Figure 11**).

The P 2p signal corresponds to phosphorous in phosphate chain and the values of the P $2p_{3/2}$ component of the phosphorous signals of the wear scars are shown in **Table 3**. A peak attributed to Zn 3s also is detected at 140.1 – 140.6 ± 0.1 eV which is considered to calculate the quantification data (elemental atomic concentration) due to the approximately same inelastic mean free path value of this peak as phosphorus and similar to the oxygen and sulphur [6, 48]. The S 2p spectra have signal in the oxidation state of -2 (Sll) which is assigned to sulphides [49] as organic and metal sulphide (ZnS here at the very top surface) and sulphur which is substituted for oxygen in the phosphate chain forming (polythio)phosphate (O-P-O → O-P-S) [50]. Using XPS is not possible to conclusively distinguish between (thio)phosphate and metal sulphide.

The modified Auger parameter (α'= Zn $2p_{3/2}$ (BE) + Zn $L_3M_{4,5}M_{4,5}$ ^1G (KE)) is calculated using the zinc $2p_{3/2}$ signal. The zinc 2p and zinc 3s might not be a decisive and self-sufficient signals in order to distinguish between zinc oxide and zinc sulphide. On the other hand, modified Auger parameter (α') and Wagner plot [51, 52] derived from Zn 2p and Zn $L_3M_{4,5}M_{4,5}$ are strong features in order to inspect the zinc chemical status. The α' for ZnO is reported to be 2009.5 – 2010.5 eV while to be 2010.1 - 2011.4 eV for ZnS [53, 54]. The values of 2009.8 - 2010.2 ± 0.2 eV for α' in this study could be an indication that the most of the zinc is present as ZnO rather than ZnS in agreement with the XANES study of similar tribofilms [55, 56].

The phosphate chain length in the ZDDP-derived tribofilm is assumed to be an important factor in determining its anti-wear performance [6, 37]. The BO/NBO ratio has been widely used to evaluate the chain length of zinc phosphate glasses [57]. However, the BO/NBO ratio may be affected by contaminants or overlaps with the peaks from other components. Hydroxides and C=O (carbonyl and carbonate) can contribute to NBO peak [6, 47] and P-O-C can contribute to BO peaks [58]. Also, the adsorbed water at 533.3-434.3 eV can bring about errors in the BO/NBO ratio [45].

Table 3. Binding energy values of the elements/compounds of the tribofilm and atomic concentration of the Zn, S and O normalised to P

	Temperature	**90°C**		**75°C**			
		a)	b)	c)	d)	e)	f)
	Lubricant: BO + ZDDP +	-	1% Water	-	1% Water	(RH 60%)	(RH 90%)
Binding energy	P $2p_{3/2}$ (eV)	133.56 ± 0.24	133.3 ± 0.08	133.52 ± 0.13	133.31 ± 0.04	133.34 ± 0.03	133.1 ± 0.07
	S $2p_{3/2}$ (eV)	162.22 ± 0.24	162.0 ± 0.1	162.15 ± 0.15	162.01 ± 0.07	162.0 ± 0.1	161.9 ± 0.1
	Zn $L_3M_{4,5}M_{4,5}$ ^1G BE (eV)	499.18 ± 0.08	Not measured	499.28 ± 0.12	498.83 ± 0.07	498.69 ± 0.08	498.70 ± 0.13
	Zn 3s - P $2p_{3/2}$ BE difference (eV)	6.85 ± 0.05	7.05 ± 0.02	6.88 ± 0.02	6.95 ± 0.02	6.97± 0.01	6.94 ± 0.03
	Zn modified Auger parameter	2010.18 ± 0.12	Not measured	2009.88 ± 0.06	2010.16 ± 0.08	2010.19 ± 0.07	2010.22 ± 0.1
	BO/NBO ratio	0.22 ± 0.02	0.20 ± 0.02	0.18 ± 0.05	0.15 ± 0.01	0.12 ± 0.04	0.12 ± 0.02
Atomic concentration	Zn/P	1.07 ± 0.07	1.84 ± 0.1	1.12 ± 0.15	1.73 ± 0.1	2.01 ± 0.2	2.14 ± 0.08
	$S_{(II)}$/P	0.71 ± 0.08	1.09 ± 0.06	0.58 ± 0.02	0.96 ± 0.13	1.32 ± 0.05	1.27± 0.09
	$O_{(phosphate)}$/P	1.75 ± 0.12	2.67 ± 0.2	1.96 ± 0.36	2.93 ± 0.22	2.32 ± 0.43	3.27 ± 0.33

The maximum error for the measurements of the signal binding energies was ± 0.1 eV. The decimal digits in the table indicate the maximum deviation from the mean value of two fitted spectra (average of measurements on two specimens)

Therefore, considering BO/NBO ratio for phosphate chain length estimation may bring about uncertainties and thus complementary parameters are required to confirm the change in the phosphate chain length. The higher ratio of the cations (Zn and Fe) to phosphorous [58]

together with the increase in the O/P ratio in the zinc (poly)phosphate can suggest a greater metal (Zn and Fe) oxide to P_2O_5 mole fraction which infers shorter (poly)phosphate chain development [57]. Also, with the more metal oxide fraction, a lower BO/NBO ratio and a shift of P $2p_{3/2}$ binding energy to lower values have been observed [45, 59-61]. As far as the ZDDP-tribofilms in this study are concerned, the tribofilms generated after 10^6 contact cycles are not expected to consist of long (poly)phosphate chains considering P $2P_{3/2}$ binding energy values (133.1 - 133.6 ± 0.1 eV) and BO/NBO ratios of 0.12 - 0.22, since P $2P_{3/2}$ in the pure long chain zinc polyphosphate appears at 134 - 135 eV [62-64].

In order to eliminate the error which may arise from the calibration and sample charging, the comparison of the (poly)phosphate chain length is also made through energy difference between Zn 3s and P $2p_{3/2}$ peaks (Zn 3s - P $2p_{3/2}$). The Zn 3s - P $2p_{3/2}$ binding energy difference tends to increase with the decrease in the (poly)phosphate chain length [65]. In addition, with an increase in the zinc phosphate chain length a decrease in the modified Auger parameter (α') binding energy was observed [45, 66].

Accordingly, to overcome the uncertainty around BO/NBO ratio, four parameters have been used in the current study; which are BO/NBO ratio, change in the ratio of Zn/P and O/P, Zn 3s - P $2p_{3/2}$ binding energy difference and Zn modified Auger parameter (α') to investigate the effect of water and humid environment on the (poly)phosphate chain length.

As can be seen in **Table 3** (a and b), decrease in BO/NBO ratio, increase in Zn/P and $O_{(phosphate)}$/P ratio and Zn 3s - P $2p_{3/2}$ BE difference suggest that 1% of added-water decreases the (poly)phosphate chain length in the ZDDP-derived tribofilm in agreement with the previous report [6].

Also, shown in **Table 3** (c,d,e and f), a decrease in BO/NBO ratio, increase in Zn/P and $O_{(phosphate)}$/P ratio, Zn 3s - P $2p_{3/2}$ BE difference and the modified Auger parameter (α') can be observed in the tribofilms derived from the lubricants containing added-water or dissolved-water absorbed through humid environments. This suggests that the dissolved-water which is absorbed into the lubricant through added-water or humid environment can decrease the (poly)phosphate chain length in the ZDDP-derived tribofilms.

IV.II The tribofilm thickness and elemental distribution

In order to estimate the tribofilm thickness and inspect the elemental distribution of the tribofilm in the wear scar, the tribofilms are sputtered using an Ar^+ ion source. Although the XPS Ar^+ ion sputtering is a valuable technique to observe the elemental distribution through

the tribofilm depth, chemical substances could be altered through preferential sputtering and intermixing the compounds [67] especially in the case of transition metals. In the case of iron, iron oxides can undergo reduction to other oxidation states [68, 69]. Therefore, loss of analysis resolution is expected through depth profiling.

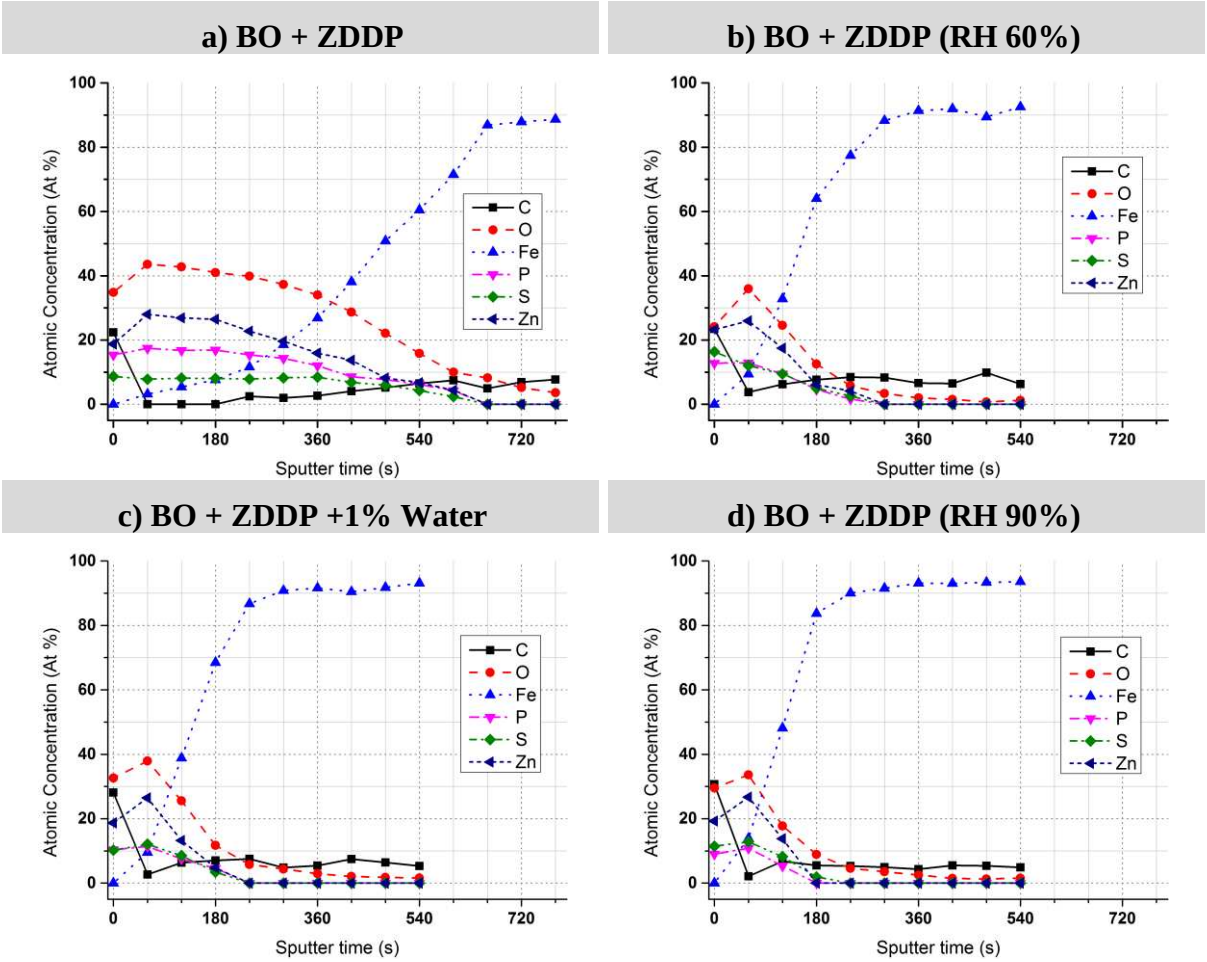

Figure 12. Sputter depth profile of the tribofilms in the wear scars lubricated with a) BO + ZDDP, b) BO + ZDDP (RH 60%), c) BO + ZDDP + 1%water and d) BO + ZDDP (RH 90%) lubricants at 75°C

The sputtered profiles of the tribofilms are shown in **Figure 12**. The sputtering and spectra acquisition between the sputtering steps have been performed in exactly same conditions for all the tribofilms shown in **Figure 12**. Also, it has been assumed that the impact of the chemical modification of the tribofilms, induced by water in oil, on sputtering rate is negligible. The tribofilm thicknesses are 12, 6, 5 and 4 minutes of the etching for the surfaces lubricated with BO + ZDDP, BO + ZDDP (RH 60%), BO + ZDDP + 1%water and BO + ZDDP (RH 90%), respectively. This shows that the dissolved-water absorbed into the lubricant through added-water or humid environments decreases the tribofilm thickness in agreement with the previous reports [3, 6].

As can be seen in **Figure 12**, the phosphorous concentration decreases from approximately 18% to around 10-12% as a consequence of added-water and humidity. Also, the atomic concentration ratio of phosphorous-to-sulphur is significantly decreased throughout the tribofilm depth suggesting contribution of inferior (poly)phosphate to the bulk of the tribofilms of the lubricants with added-water and tests under humid environments.

5. Discussion

I. The effect of dissolved-water

Figure 13 is plotted using the information provided in **Figure 4**, **Figure 6, Figure 8, Figure 12** and **Table 3** relative to the increase in the water saturation level at 75°C. The micropitted surface area proportionally increases with an increase in water saturation level. Also, increase in water saturation level in the lubricant brings about a decrease in the ZDDP-tribofilm thickness and P $2p_{3/2}$ binding energy. The effect of water and humid environments on decreasing the ZDDP-tribofilm thickness and phosphorous binding energy has also been reported previously [3, 6]. Furthermore, the presence of abrasive marks in the wear scars of lubricants is enhanced in respect to an increase in dissolved-water level (**Figure 3**, **Figure 4** and **Figure 6)**.

The decrease in phosphorous binding energy can be explained considering the increase in O/P ratio in the (poly)phosphate chain (see **Figure 13** a) which leads to an increase in partial positive charge on each phosphorous atoms [70]. Therefore, decrease in P $2p_{3/2}$ binding energy implies the presence of shorter chain (poly)phosphate in the ZDDP-tribofilms of the lubricants with dissolved-water. As can be seen in **Figure 13** (a and b) the ZDDP-tribofilms generated under humid environments and from lubricants with added-water have inferior BO/NBO ratio, greater ratios of Zn/P and O/P, higher Zn 3s - P $2p_{3/2}$ binding energy difference and greater α' values which confirm the effect of dissolved-water on decreasing the poly(phosphate) chain length in the ZDDP-tribofilm. The wear scar of the roller lubricated with BO + ZDDP (RH 90%) which has the highest level of the dissolved-water has the shortest (poly)phosphate chain length considering least P $2p_{3/2}$ binding energy and BO/NBO ratio and significant increase in the O/P ratio.

The ZDDP-tribofilm enhances micropitting incidences at the contact zone having highest contact pressure and promotes micropitting propagation. On the other hand, the ZDDP-tribofilm is an interfacial layer which assists in maintaining the contact bodies separated and accommodating contact pressure. Therefore, the thinner ZDDP-tribofilm leads to a higher

probability of asperity-asperity contacts and consequently promotes micropitting nucleation. Also, mild wear at the edge of the wear scars of the lubricants with the dissolved-water increases the contact area which leads to nucleation of micropits across the wear scar and expansion of the micropitting nucleation to the edge of wear scar. As observed in **Figure 3**, **Figure 4** and **Figure 6** micropitting nucleating is enhanced in the presence of water and humidity and micropits can be observed spread out across the wear scars showing deteriorated action of the tribofilms in preventing asperity–asperity contact.

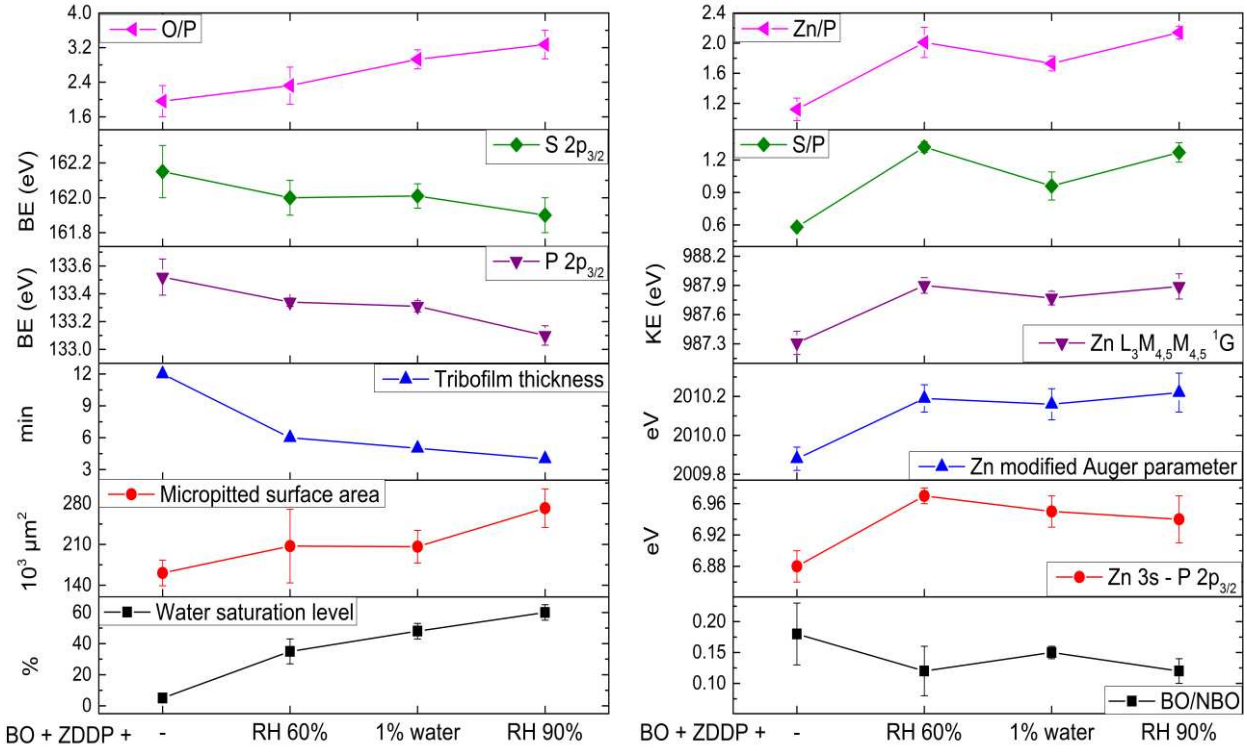

Figure 13. The effect of water and humid environments on micropitting and relevant tribochemistry at 75°C

The enhancing impact of water and humidity on mild wear at the edge of the wear scar and abrasive wear can be explained by the hard and soft acids and bases (HSAB) theory which is established by Ho and Pearson [71, 72] and well-implemented to ZDDP by Martin [57]. Abrasive wear can be induced through hard metallic oxide (iron-oxide) wear particles in the lubricant which are originated from the steel substrate. Iron-oxide is a harder Lewis acid compared to zinc-oxide in zinc (poly)phosphate glass. Therefore, in compliance with HSAB the zinc (poly)phosphate glass can eliminate iron-oxide wear particles through a chemical reaction. In addition, the thicker and longer-chain (poly)phosphate (hard base) in the ZDDP-tribofilm has a superior potential to digest iron-oxide wear particles and avoid abrasive wear

compared to a thinner and shorter-chain (poly)phosphate. Water and humidity induce thinner and shorter-chain (poly)phosphate ZDDP-tribofilm.

As far as the ZDDP molecule in the lubricant is concerned, water in the lubricant can attack to the zinc atom and induce a hydrolytic reaction [20, 73, 74]. The rate of hydrolysis depends on the size and nature of the alkyl group (primary or secondary) [74] and the lubricant polarity which affect the availability of the zinc atom to the water attack. The final product of the hydrolytic reaction can be phosphoric acid [73, 74] which hinders polyphosphate formation. Therefore, tribofilm formation in the presence of water is mitigated through hydrolytic effect of water leading to a thinner tribofilm formation in the presence of water.

Furthermore, it has been suggested that absorbed water in the lubricant depolymerise the long-chain (poly)phosphate in the thermal/tribo film to the short-chain (poly)phosphate [21]. This can be the case especially in the event of high contact pressure and shear stress [60, 65]. As can be seen in **Figure 8,** the absorbed water to some extent is present in the BO + ZDDP lubricants (tests in laboratory condition) throughout the tests which can have a catalytic influence on short-chain (poly)phosphate formation. Thereby, an increase in the dissolved-water level accelerates water hydrolytic effect leading to a shorter-chain (poly)phosphate.

Also, as can be seen in **Figure 12** the phosphorus concentration, corresponding to (poly)phosphate, is significantly decreased throughout the depth of ZDDP-tribofilms with dissolved-water. A thinner ZDDP-tribofilm formation having a shorter chain (poly)phosphate with less (poly)phosphate contribution to the tribofilm bulk is the reason behind emergence of the abrasive wear and mild wear at the edge of the wear scars lubricated with the lubricants containing added-water or under humid environments.

A higher ratio of Zn/P and S/P in the ZDDP-tribofilm induced under humid environments and lubricants with added-water can be observed in **Figure 13** implying enhanced formation of ZnS in the ZDDP-tribofilms of the lubricants with dissolved-water [6]. The Zn $L_3M_{4,5}M_{4,5}\,^1G$ in ZnS appears at higher Kinetic Energies (KE) (lower binding energies) compared to ZnO [49, 53], thereby increase in Zn $L_3M_{4,5}M_{4,5}\,^1G$ (KE) (**Figure 13**) is an indication of enhanced ZnS formation. Also, an increase in α' in Wagner plot also can suggest that ZnS formation is partly enhanced [53]. The Zn/P and S/P ratio alter with a similar trend with respect to the dissolved-water level. In addition, Zn $L_3M_{4,5}M_{4,5}\,^1G$ (KE) and Zn modified Auger parameter (α') follow similar trend to that of Zn/P and S/P ratios (see **Figure 13**). The trend observed for Zn/P and S/P ratios, Zn $L_3M_{4,5}M_{4,5}\,^1G$ (KE) and α' shows greater ZnS formation in the ZDDP-tribofilm

of the lubricants with dissolved-water. Also, it can be implied that effect of humidity on enhancing ZnS formation is more influential than that of added-water in the test conditions used in this study. The importance of ZnO in the ZDDP-tribofilm and ZDDP-thermally decomposition products can be addressed due to its ability to inhibit ZDDP hydrolysis [75, 76].

Although an increase in Zn 3s - P $2p_{3/2}$ BE difference for the lubricants with dissolved-water is an indication of a shorter (poly)phosphate chain, as can be seen in **Figure 13**, the Zn 3s - P $2p_{3/2}$ BE difference is not following the trend of P $2p_{3/2}$ BE. This is arisen from the change in the zinc states which affects the Zn 3s binding energy. Therefore, the Zn 3s - P $2p_{3/2}$ BE difference is influenced by the change in (poly)phosphate chain length and zinc states, thus in the lubricant formulations where a shift in the zinc states is expected, the Zn 3s - P $2p_{3/2}$ BE difference is not a self-sufficient parameter in order to determine the (poly)phosphate chain length.

II. The effect of free-water

In contrast to dissolved-water condition, almost no or negligible micropitting is observed in free-water condition. As shown, dissolved-water prompts thinner ZDDP-derived tribofilm formation and enhances mild and abrasive wear. In free-water condition ZDDP-derived tribofilm formation is totally hindered and mild wear exceeds micropitting wear. Therefore, micropitting propagation is suppressed and nucleated micropits will be immediately worn out by the accelerated mild wear. This mechanism of micropitting elimination by mild wear is schematically presented in **Figure 14**.

Thereby, the negligible micropits on the roller surface lubricated in free-water condition are initiated micropits which are either not eliminated by mild-wear or generated within the stopping-step. Extending the tribological contact to 10^6 contact cycles, the water saturation level fell below 100% and dissolved-water condition will dominate the contact. As observed in **Figure 10** (b) micropitting is enhanced under dissolved-water conditions and the lubricant with a greater dissolved-water, resulted from BO+ZDDP+3%water lubricant, shows significantly intensified micropitting in the wear scar.

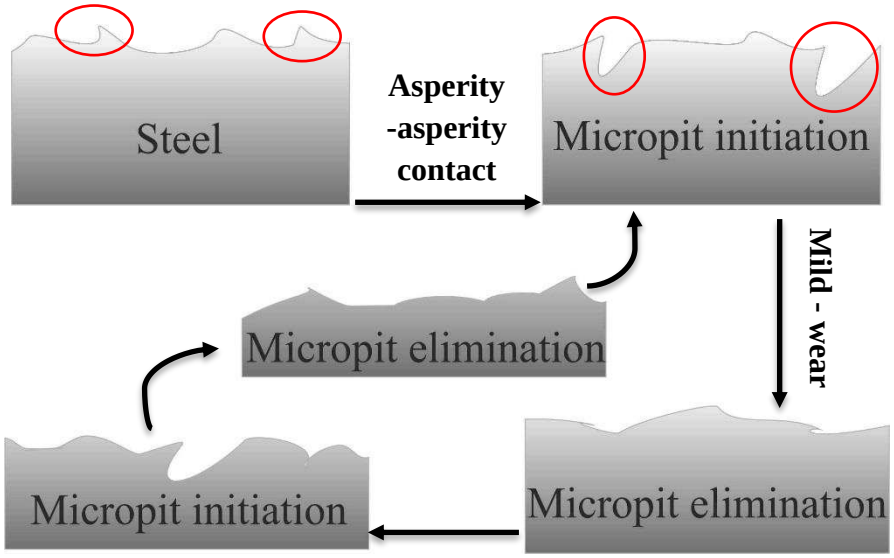

Figure 14. Immediate elimination of the initiated micropits by mild-wear in free-water condition.

6. Conclusions

The tribocorrosive influence of water and relative humidities on micropitting under boundary lubricated rolling/sliding contacts is studied mechanistically using a specially modified MPR for understanding tribocorrosion systems. Using WLI a promising procedure for micropitting mapping is implemented in order to achieve a micropitting surface area. The micropits propagate opposite to the sliding direction into the material bulk and also transverse to the rolling/sliding direction. The tribocorrosive wear and micropitting nucleation are enhanced with increased dissolved-water level in PAO + ZDDP lubricant formulation as the consequences of the tribochemical changes in the tribofilms. From this work following conclusions can be drawn:

- The micropitting surface area and abrasive wear proportionally increase with an increase of dissolved-water level in the lubricant absorbed through added-water or humid environments.
- The ZDDP-tribofilm thickness and (poly)phosphate chain length are inversely proportional to the dissolved-water level in the lubricant. Also, water and humidity alter the ZnO/ZnS ratio in the ZDDP-tribofilm to a certain extent.
- The thinner ZDDP-tribofilm formation in the presence of dissolved-water enhances micropitting nucleation due to greater asperity-asperity contacts.

- Water and humidity favours mild wear through interfering with ZDDP-tribofilm formation. Thinner ZDDP-tribofilm, shorter (poly)phosphate chain and less contribution of phosphate to the bulk of ZDDP-tribofilm induced by dissolved-water are the reasons behind enhanced mild and abrasive wear.
- While dissolved-water increases micropitting nucleation and expands the nucleation across the wear scar, in free-water condition micropitting appearance is suppressed due to a dominant action of the mild wear.

7. Acknowledgements

This study was funded by the FP7 program through the Marie Curie Initial Training Network (MC-ITN) entitled "FUTURE-BET-Formulating an Understanding of Tribocorrosion in ArdUous Real Environments – Bearing Emerging Technologies" (317334) and was carried out at University of Leeds and SKF Engineering and Research Centre. The authors would like to thank to all FUTURE-BET partners whom had kind discussions on the topic and the methodology.

8. References

[1] Schatzberg P, Felsen IM. Effects of water and oxygen during rolling contact lubrication. Wear. 1968;12:331-42.

[2] Fitch J, Jaggernauth S. MOISTURE--The Second Most Destructive Lubricant Contaminate, and its Effects on Bearing Life. P/PM Technology. 1994;12:1-4.

[3] Cen H, Morina A, Neville A, Pasaribu R, Nedelcu I. Effect of water on ZDDP anti-wear performance and related tribochemistry in lubricated steel/steel pure sliding contacts. Tribol Int. 2012;56:47-57.

[4] Goto H, Buckley D. The influence of water vapour in air on the friction behaviour of pure metals during fretting. Tribol Int. 1985;18:237-45.

[5] Lancaster J. A review of the influence of environmental humidity and water on friction, lubrication and wear. Tribol Int. 1990;23:371-89.

[6] Nedelcu I, Piras E, Rossi A, Pasaribu H. XPS analysis on the influence of water on the evolution of zinc dialkyldithiophosphate–derived reaction layer in lubricated rolling contacts. Surface and Interface Analysis. 2012;44:1219-24.

[7] Parsaeian P, Ghanbarzadeh A, Wilson M, Van Eijk MC, Nedelcu I, Dowson D, Neville A, Morina A. An experimental and analytical study of the effect of water and its tribochemistry on the tribocorrosive wear of boundary lubricated systems with ZDDP-containing oil. Wear. 2016;358:23-31.

[8] Troyer D. The Visual Crackle-A New Twist to an Old Technique. Practicing Oil Analysis magazine. 1998.

[9] Needelman WM, Barris MA, LaVallee GL. Contamination control for wind turbine gearboxes. Power Engineering. 2009;113:112-20.

[10] Stachowiak G, Batchelor AW. Engineering tribology: Butterworth-Heinemann; 2013.

[11] Stadler K, Stubenrauch A. Premature bearing failures in industrial gearboxes. Antriebstechnisches Kolloquium (ATK)2013. p. 19-20.

[12] Cantley RE. The effect of water in lubricating oil on bearing fatigue life. ASLE TRANSACTIONS. 1977;20:244-8.

[13] Strandell I, Fajers C, Lund T. Corrosion—One Root Cause for Premature Failures. 37th Leeds-Lyon symposium on tribology2010.

[14] Schatzberg P. Inhibition of water-accelerated rolling-contact fatigue. Journal of Lubrication Technology. 1971;93:231-3.

[15] Matsumoto Y, Murakami Y, Oohori M. Rolling contact fatigue under water-infiltrated lubrication. Bearing steel technology: ASTM International; 2002.

[16] Ruellan A, Cavoret J, Ville F, Kleber X, Liatard B. Understanding white etching cracks in rolling element bearings: State of art and multiple driver transposition on a twin-disc machine. Proceedings of the Institution of Mechanical Engineers, Part J: Journal of Engineering Tribology. 2016:1350650116648058.

[17] Schatzberg P, Felsen IM. Influence of water on fatigue-failure location and surface alteration during rolling-contact lubrication. Journal of Lubrication Technology. 1969;91:301-7.

[18] Magalhaes J, Ventsel L, MacDonald D. Environmental effects on pitting corrosion of AISI 440C ball bearing steels: Experimental results©. Lubr Eng. 1999;55:36-41.

[19] Rounds FG. Additive interactions and their effect on the performance of a zinc dialkyl dithiophosphate. Asle Transactions. 1978;21:91-101.

[20] Spedding H, Watkins R. The antiwear mechanism of zddp's. Part I. Tribol Int. 1982;15:9-12.

[21] Fuller MLS, Kasrai M, Bancroft GM, Fyfe K, Tan KH. Solution decomposition of zinc dialkyl dithiophosphate and its effect on antiwear and thermal film formation studied by X-ray absorption spectroscopy. Tribol Int. 1998;31:627-44.

[22] Fatima N, Minami I, Holmgren A, Marklund P, Larsson R. Surface chemistry of wet clutch influenced by water contamination in automatic transmission fluids. Tribol Int. 2016;96:395-401.

[23] Fatima N, Minami I, Holmgren A, Marklund P, Berglund K, Larsson R. Influence of water on the tribological properties of zinc dialkyl-dithiophosphate and over-based calcium sulphonate additives in wet clutch contacts. Tribol Int. 2015;87:113-20.

[24] McDONALD RA. Zinc dithiophosphates. CHEMICAL INDUSTRIES-NEW YORK-MARCEL DEKKER-. 2003:29-44.

[25] Costa HL, Spikes HA. Impact of ethanol on the formation of antiwear tribofilms from engine lubricants. Tribol Int. 2016;93, Part A:364-76.

[26] Wu X, Zhang J, Qi W, Gu X, Zhang L. The effect of SP gear oil on load capacity of carburized gears. In: MCI P, FRANCE (1999), editor. 4th World congress on gearing and power transmission Paris, France 1999.

[27] Hong HS, Huston M, O'Connor B, Stadnyk N. Evaluation of surface fatigue performance of gear oils. Lubr Sci. 1998;10:365-80.

[28] Tuszynski W. An effect of lubricating additives on tribochemical phenomena in a rolling steel four-ball contact. Tribol Lett. 2006;24:207-15.

[29] Johansson J, Devlin MT, Prakash B. Lubricant additives for improved pitting performance through a reduction of thin-film friction. Tribol Int. 2014;80:122-30.

[30] Wan G, Amerongen E, Lankamp H. Effect of extreme-pressure additives on fatigue life of rolling bearings. J Phys D: Appl Phys. 1992;25:147-53.

[31] Torrance A, Morgan J, Wan G. An additive's influence on the pitting and wear of ball bearing steel. Wear. 1996;192:66-73.

[32] Pasaribu H, Lugt P. The composition of reaction layers on rolling bearings lubricated with gear oils and its correlation with rolling bearing performance. Tribol Trans. 2012;55:351-6.

[33] Laine E, Olver A, Beveridge T. Effect of lubricants on micropitting and wear. Tribol Int. 2008;41:1049-55.

[34] Brizmer V, Pasaribu H, Morales-Espejel GE. Micropitting performance of oil additives in lubricated rolling contacts. Tribol Trans. 2013;56:739-48.

[35] Morales-Espejel GE, Brizmer V. Micropitting modelling in rolling–sliding contacts: Application to rolling bearings. Tribol Trans. 2011;54:625-43.

[36] Soltanahmadi S, Morina A, van Eijk MCP, Nedelcu I, Neville A. Investigation of the effect of a diamine-based friction modifier on micropitting and the properties of tribofilms in rolling-sliding contacts. Journal of Physics D: Applied Physics. 2016;49:505302.

[37] Spikes H. The history and mechanisms of ZDDP. Tribol Lett. 2004;17:469-89.

[38] Errichello R. Morphology of Micropitting. AGMA 11FTM17. 2011.

[39] Devlin M, Ryan H, Tsang V, Corbett P, Strand L, Turner TL, Wallo C, Jao T-C. The effect of water contamination and oxidation on the fatigue life performance of wind turbine lubricants. NLGI Spokesman-Including NLGI Annual Meeting-National Lubricating Grease Institute: [Kansas City, Mo.] National Lubricating Grease Institute.; 2004. p. 22-30.

[40] Sheng S. Wind turbine micropitting workshop: a recap: National Renewable Energy Laboratory; 2010.

[41] Oila A, Bull S. Assessment of the factors influencing micropitting in rolling/sliding contacts. Wear. 2005;258:1510-24.

[42] Hamrock BJ, Dowson D. Isothermal elastohydrodynamic lubrication of point contacts: Part III—Fully flooded results. J Tribol. 1977;99:264-75.

[43] Sonntag RE, Borgnakke C, Van Wylen GJ, Van Wyk S. Fundamentals of thermodynamics: Wiley New York; 1998.

[44] Chastain J, King RC, Moulder J. Handbook of X-ray photoelectron spectroscopy: a reference book of standard spectra for identification and interpretation of XPS data: Physical Electronics Eden Prairie, MN; 1995.

[45] Crobu M, Rossi A, Mangolini F, Spencer ND. Chain-length-identification strategy in zinc polyphosphate glasses by means of XPS and ToF-SIMS. Analytical and bioanalytical chemistry. 2012;403:1415-32.

[46] Oila A, Bull S. Phase transformations associated with micropitting in rolling/sliding contacts. Journal of materials science. 2005;40:4767-74.

[47] Martin J, Grossiord C, Le Mogne T, Igarashi J. Role of nitrogen in tribochemical interaction between Zndtp and succinimide in boundary lubrication. Tribol Int. 2000;33:453-9.

[48] Seah M, Dench W. Quantitative electron spectroscopy of surfaces. Surface and interface analysis. 1979;1:2-11.

[49] Brion D. Etude par spectroscopie de photoelectrons de la degradation superficielle de FeS 2, CuFeS 2, ZnS et PbS a l'air et dans l'eau. Applications of Surface Science. 1980;5:133-52.

[50] Martin JM, Grossiord C, Le Mogne T, Bec S, Tonck A. The two-layer structure of Zndtp tribofilms: Part I: AES, XPS and XANES analyses. Tribol Int. 2001;34:523-30.

[51] Wagner C. Auger lines in x-ray photoelectron spectrometry. Analytical Chemistry. 1972;44:967-73.

[52] Moretti G. Auger parameter and Wagner plot in the characterization of chemical states by X-ray photoelectron spectroscopy: a review. Journal of electron spectroscopy and related phenomena. 1998;95:95-144.

[53] Deroubaix G, Marcus P. X-ray photoelectron spectroscopy analysis of copper and zinc oxides and sulphides. Surface and Interface Analysis. 1992;18:39-46.

[54] Dake L, Baer D, Zachara J. Auger parameter measurements of zinc compounds relevant to zinc transport in the environment. Surface and Interface Analysis. 1989;14:71-5.

[55] Zhang Z, Yamaguchi E, Kasrai M, Bancroft G, Liu X, Fleet M. Tribofilms generated from ZDDP and DDP on steel surfaces: Part 2, chemistry. Tribol Lett. 2005;19:221-9.

[56] Yin Z, Kasrai M, Fuller M, Bancroft GM, Fyfe K, Tan KH. Application of soft X-ray absorption spectroscopy in chemical characterization of antiwear films generated by ZDDP Part I: the effects of physical parameters. Wear. 1997;202:172-91.

[57] Martin JM. Antiwear mechanisms of zinc dithiophosphate: a chemical hardness approach. Tribol Lett. 1999;6:1-8.

[58] Rossi A, Piras F, Kim D, Gellman A, Spencer N. Surface reactivity of tributyl thiophosphate: effects of temperature and mechanical stress. Tribol Lett. 2006;23:197-208.

[59] Liu H, Chin T, Yung S. FTIR and XPS studies of low-melting PbO-ZnO-P 2 O 2 glasses. Materials chemistry and physics. 1997;50:1-10.

[60] Crobu M, Rossi A, Mangolini F, Spencer ND. Tribochemistry of bulk zinc metaphosphate glasses. Tribol Lett. 2010;39:121-34.

[61] Heuberger RC. Combinatorial study of the tribochemistry of anti-wear lubricant additives: Diss., Eidgenössische Technische Hochschule ETH Zürich, Nr. 17207, 2007; 2007.

[62] Onyiriuka E. Zinc phosphate glass surfaces studied by XPS. Journal of non-crystalline solids. 1993;163:268-73.

[63] Brow RK, Tallant DR. Structural design of sealing glasses. Journal of Non-Crystalline Solids. 1997;222:396-406.

[64] Eglin M, Rossi A, Spencer ND. X-ray photoelectron spectroscopy analysis of tribostressed samples in the presence of ZnDTP: a combinatorial approach. Tribol Lett. 2003;15:199-209.

[65] Crobu M, Rossi A, Spencer ND. Effect of chain-length and countersurface on the tribochemistry of bulk zinc polyphosphate glasses. Tribol Lett. 2012;48:393-406.

[66] Eglin M. Development of a combinatorial approach to lubricant additive characterization: Diss., Technische Wissenschaften ETH Zürich, Nr. 15054, 2003; 2003.

[67] Wagner C, Briggs D, Seah M. Practical surface analysis. Auger and X-ray Photoelectron Spectroscopy. 1990;1:595.

[68] Lad RJ, Henrich VE. Structure of α-Fe 2 O 3 single crystal surfaces following Ar+ ion bombardment and annealing in O 2. Surface Science. 1988;193:81-93.

[69] Mills P, Sullivan J. A study of the core level electrons in iron and its three oxides by means of X-ray photoelectron spectroscopy. Journal of Physics D: Applied Physics. 1983;16:723.

[70] Beletskii I, Yatsimirskii K. Electronic structure of polyphosphate ions. Theoretical and Experimental Chemistry. 1988;23:621-7.

[71] Ho T-L. Hard soft acids bases (HSAB) principle and organic chemistry. Chemical Reviews. 1975;75:1-20.

[72] Pearson RG. Chemical hardness: Wiley-VCH; 1997.

[73] BURN A, DEWAN S, GOSNEY I, TAN P. 31P NMR Study of the Mechanism and Kinetics of the Hydrolysis of Zinc (II) O, O-Diethyl Dithiophosphate and Some Related Compounds. ChemInform. 1990;21.

[74] Burn AJ, Gosney I, Warrens CP, Wastle JP. Phosphorus-31 NMR investigation of the heterogeneous hydrolytic decomposition of zinc (II) bis (O, O-dialkyl dithiophosphate) lubricant additives. Journal of the Chemical Society, Perkin Transactions 2. 1995:265-8.

[75] Burn AJ, Dewan SK, Gosney I, Tan PS. Inhibition of hydrolysis of ‘normal’zinc (II) O, O′-di-isopropyl dithiophosphate by the ‘basic’form. Journal of the Chemical Society, Perkin Transactions 2. 1990:1311-6.

[76] Harrison PG, Kikabhai T. Proton and phosphorus-31 nuclear magnetic resonance study of zinc (II) O, O′-dialkyl dithiophosphates in solution. Journal of the Chemical Society, Dalton Transactions. 1987:807-14.